ACS Macro Letters

pubs.acs.org/macroletters Letter

UV Irradiation-Induced Cyclic-to-Linear Topological Changes of a Light/pH Dual-Sensitive Cyclic Copolymer for Enhanced Drug Delivery

Hongbing Liu,[§] Zheng Guo,[§] Wei Ma, Shuang Li, Dun Wang, Zhi Zheng, Ying Liu, Cui-Yun Yu,* and Hua Wei*

Cite This: *ACS Macro Lett.* 2023, 12, 1025−1030 Read Online

ACCESS | Metrics & More | Article Recommendations | Supporting Information

ABSTRACT: Cyclic polymers with cleavable backbones triggered by either external or internal stimuli can realize simultaneous extracellular stability and intracellular destabilization of cyclic polymer-based nanocarriers but remain seldom reported. To this end, we prepared herein cyclic-ONB-P(OEGMA-*st*-DMAEMA) (*c*-ONB-P(OEGMA-*st*-DMAEMA)) with a light-cleavable junction in the polymer backbone based on oligo (ethylene glycol) monomethyl ether methacrylate (OEGMA) and N,N-dimethylaminoethyl methacrylate (DMAEMA) using a light-cleavable atom transfer radical polymerization (ATRP) initiator containing an o-nitrobenzyl (ONB) ester group. Together with the pH-sensitivity of DMAEMA, *c*-ONB-P(OEGMA-*st*-DMAEMA) shows a light-cleavable mainchain and pH-sensitive side chains. Notably, doxorubicin (DOX)-loaded *c*-ONB-P(OEGMA$_4$-st-DMAEMA$_{38}$) (C2) micelles mediated an IC_{50} value of 2.28 μg/mL in Bel-7402 cells, which is 1.7-fold lower than that acquired without UV irradiation. This study thus reported the synthesis of a cyclic copolymer with a UV-cleavable backbone and uncovered the effects of topological modulation on the in vitro controlled release properties of cyclic polymers.

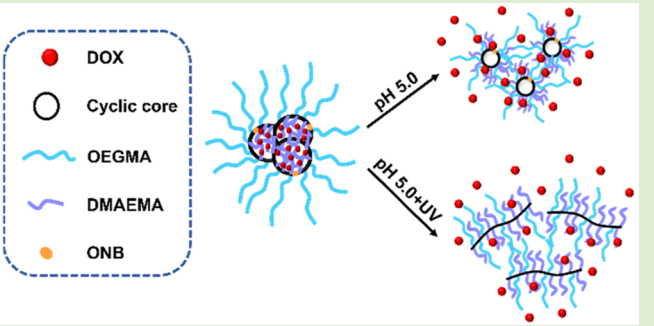

Polymeric micelles represent probably one of the most studied nanocarriers for anticancer drug delivery owing to their notable advantages.[1−3] However, compromised micelle stability in the blood circulation upon intravenous injection due to massive dilution by body fluids and blood and interactions with a variety of biomolecules and extraneous factors leads to leakage and premature diffusion of encapsulated therapeutics resulting in toxicity to normal tissues and significantly compromised therapeutic efficiency at the focal site.[4,5] Polymers with advanced topologies, including star-shaped,[6,7] (hyper)branched,[8] dendritic,[9] bottlebrush,[10] and cyclic structures,[11,12] have been reported to endow the resulting polymeric self-assemblies with enhanced colloidal stability for long blood circulation in vivo. Among these reported advanced topological architectures, cyclic and its derived topologies have attracted considerable interest in the past decade because of the endless chain structure-associated unique properties that are quite different from those of linear counterparts.[13] Specifically, cyclic polymers have been recently highlighted to show better performance as delivery systems in comparison to linear analogues for drug delivery due to the well-documented stronger steric hindrance of a cyclic topology in comparison to that of a linear one for enhanced colloidal stability.[14−17]

Meanwhile, a stabilized nanocarrier must undergo a structural change for efficient intracellular destabilization induced by one or more external/internal triggers to exert the desired therapeutic efficiency.[18,19] In this regard, the leading strategies adopted to induce the destabilization of a cyclic polymer-based nanocarrier mainly focused on the modification and functionalization of the side chains of cyclic polymers.[20−22] Notable examples were cyclic polymers constructed with either stimuli-responsive monomers or intracellular triggers-cleavable links, which, however, inevitably led to inadequate intracellular drug release due to the lack of cyclic topology disruption.[13] A stimuli-responsive cyclic backbone is thus highly desirable for promoted intracellular drug release but remains relatively unexplored likely due to the synthetic challenge.

Exogenous photoreactive stimuli are easier to control than endogenous ones.[23] The common photoreactive groups

Received: May 8, 2023
Accepted: July 5, 2023
Published: July 11, 2023

https://doi.org/10.1021/acsmacrolett.3c00265
ACS Macro Lett. 2023, 12, 1025−1030

include azobenzene,[24] coumarin,[25] cinnamic acid,[26] and o-nitrobenzyl ester.[27] O-nitrobenzyl (ONB) ester has attracted considerable interest due to the ease of synthesis and prompt breakage properties.[28] Therefore, it will be a useful strategy to incorporate an ONB ester into the cyclic polymer backbone.

To this end, we report herein preparation of cyclic-ONB-P(OEGMA-*st*-DMAEMA) (*c*-ONB-P(OEGMA-*st*-DMAEMA)) with a light-cleavable junction in the polymer backbone based on oligo (ethylene glycol) monomethyl ether methacrylate (OEGMA) and N,N-dimethylaminoethyl methacrylate (DMAEMA) using a light-cleavable atom transfer radical polymerization (ATRP) initiator containing an o-nitrobenzyl (ONB) ester group. Together with the well-documented pH-sensitive DMAEMA units, *c*-ONB-P(OEGMA-*st*-DMAEMA) shows dual sensitivities, i.e., a light-cleavable mainchain and pH-sensitive side chains. Optimization of the polymer composition, in terms of micelle stability, was further performed. Finally, in vitro evaluations were conducted to disclose the unprecedented effects of dual sensitivity and topological modulation on the in vitro performance of cyclic copolymers for anticancer drug delivery (Scheme 1).

Scheme 1. Schematic Illustration of the Self-Assembled Micelles for Drug Encapsulation and Intracellular Drug Release Behaviors

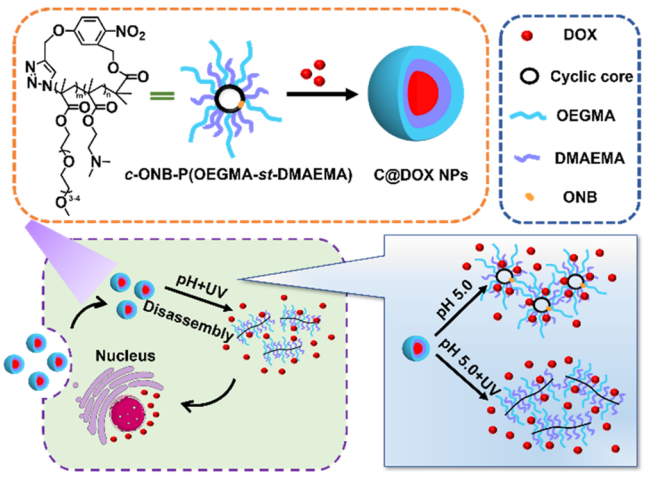

The target light/pH dual sensitive cyclic copolymer *c*-ONB-P(OEGMA-*st*-DMAEMA) was synthesized via three successive steps, including (i) preparation of a double-head initiator with a central light-cleavable ONB link by successive reduction, substitution, and esterification reactions of 5-hydroxy-2-nitrobenzaldehyde; (ii) synthesis of an α-alkyne-ω-azide linear precursor, *l*-ONB-P(OEGMA-*st*-DMAEMA)-N_3 via the light-responsive double-head initiator-mediated ATRP of OEGMA and DMAEMA followed by azidotion of the bromine chain terminus; and (iii) production of the target light/pH dual responsive cyclic copolymer, *c*-ONB-P(OEGMA-*st*-DMAEMA) by Cu(I)-catalyzed intrachain click cyclization of the linear precursor in a highly diluted condition (Figures S1 and S5).

A double-head initiator with a central light-cleavable ONB link (refer to the Supporting Information (Figures S1−S4) for the synthesis details) was first prepared. The molecular weights (MWs), polydispersity indexes (*Đ*'s), and polymer compositions of the synthesized polymers were characterized by ^{1}H NMR (Figure S6) and SEC-MALLS (Figure 1a) measurements. The degree of polymerization (DP) values of OEGMA and DMAEMA units were calculated by ^{1}H NMR data following the previously reported methods.[13]

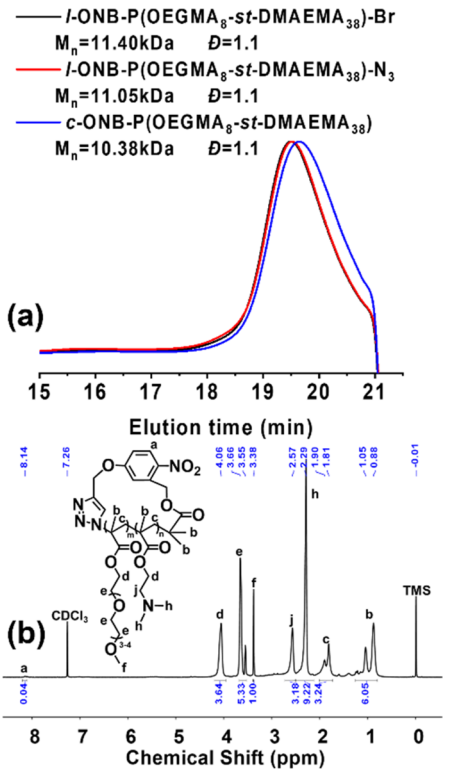

Figure 1. (a) SEC elution traces of *l*-ONB-P(OEGMA$_8$-*st*-DMAEMA$_{38}$)-Br, *l*-ONB-P(OEGMA$_8$-*st*-DMAEMA$_{38}$)-N_3, and *c*-ONB-P(OEGMA$_8$-*st*-DMAEMA$_{38}$); (b) ^{1}H NMR spectrum of *c*-ONB-P(OEGMA$_8$-*st*-DMAEMA$_{38}$)-Br in $CDCl_3$.

Successful azidation of bromine chain termini was supported by the appearance of a characteristic absorption centered at 2100 cm^{-1} assigned to the azide group in the FT-IR spectrum (Figure S7) and a discernible slight shift of the SEC elution trace of *l*-ONB-P(OEGMA-*st*-DMAEMA)-N_3 toward a longer retention time compared to that of *l*-ONB-P(OEGMA-*st*-DMAEMA)-Br (Figure 1a). Subsequent intrachain click coupling of α-alkyne-ω-azide linear precursor in an extremely diluted solution afforded a cyclic statistical copolymer, *c*-ONB-P(OEGMA-*st*-DMAEMA), which was confirmed by the significantly compromised intensity of the azide signal recorded at 2100 cm^{-1} in the FT-IR spectrum after cyclization as well as a clear right shift of the SEC elution peak of the resulting cyclized polymer to a low-molecular weight-side relative to the linear precursor because of the well-documented more compact dimension of a cyclic polymer without chain termini than that of the linear analogue (Figure 1a).[29] Further determination of the polymer composition based on the ^{1}H NMR data after cyclization confirmed an unaltered polymer composition in comparison to that of the linear precursor (Figure 1b), strongly supporting that the right shift of the SEC elution toward a lower molecular weight after cyclization was attributed substantially to the cyclic topology generation rather than polymer degradation. All of the above results confirmed the successful synthesis of the target dual-sensitive cyclic copolymer, *c*-ONB-P(OEGMA-*st*-DMAEMA). The molecular

https://doi.org/10.1021/acsmacrolett.3c00265
ACS Macro Lett. 2023, 12, 1025−1030

parameters of the synthesized polymers are summarized in Table S1.

Due to the presence of a UV-sensitive ONB ester group in the polymer backbone, the phototriggered structural dissociation of L and C was validated by ^{1}H NMR (Figures 2a,b and

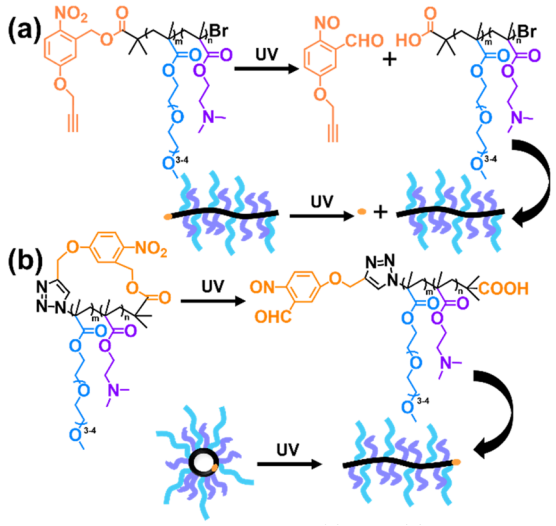

Figure 2. Chemical structure changes of (a) L and (b) C after UV light exposure.

S9), which showed the absence of the methylene proton signal at 5.5 ppm and the presence of the corresponding aldehyde proton at 9.8 ppm after UV irradiation due to the conversion of an o-nitrobenzyl ester to an aldehyde function.

Critical micelle concentration (CMC), the lowest concentration at which self-assembly of amphiphiles into micelles occurs, provides a direct insight into the colloidal stability of formed micelles with a lower one preferred for better thermodynamic micelle stability.[30] Therefore, the CMCs of L and C were determined by using a classical fluorescence probe of pyrene. In the emission spectra of pyrene, the intensity at 384 nm increased sharply with increasing polymer concentrations, indicating the transfer of pyrene from a hydrophilic medium to a hydrophobic micelle core domain for enhanced fluorescence properties. This onset polymer concentration for micelle self-assembly is thus defined as the CMC value (Figure S10). The CMC values of the C1, L1, C2, and L2 copolymers were calculated to be 0.016, 0.022, 0.012, and 0.017 mg/mL, respectively. Cyclic polymers showed CMCs lower than those of linear analogues due to the greater stability of cyclic polymers with stronger steric hindrance. C2 showed a CMC smaller than that of C1 likely due to a higher weight fraction of the hydrophobic DMAEMA moiety in the C2 structure.

Next, C- and L-based micelles (C and L micelles) were produced via a classical dialysis method at a fixed polymer concentration above the CMCs. The mean hydrodynamic diameters of the self-assembled micelles were determined to be 186.7, 172.6, 134.5, and 126.7 nm for L1, C1, L2, and C2, respectively, by dynamic light scattering (DLS) measurements (Figure S11). C micelles exhibited average sizes smaller than those of the L micelles, which agrees well with the CMC data.

The salt stability of the self-assembled C and L micelles was supported by the almost constant particle sizes in PBS (pH 7.4) compared to those recorded in water for all four micelle formulations. The structural destabilization of C and L micelles in an intracellular acidic pH mimicking condition was investigated by DLS (Figure S11). Incubation of C and L micelles at pH 5.0 for 24 h led to a dramatic decrease of the micelle sizes from 100−200 to nearly 10 nm (Figure S12), suggesting complete micelle disassembly due to the acidic pH-triggered hydrophobic to hydrophilic transformation of DMAEMA units.

The UV irradiation-triggered structural changes of the C and L micelles were further evaluated (Figure S13). As expected, L micelles showed an almost unaltered particle size upon 1 h of UV irradiation due to an insignificant effect of terminal ONB ester removal on the self-assembly properties of L micelles. In contrast, C micelles underwent an increase of approximately 20 nm in particle size in an identical condition attributed feasibly to the UV-induced cyclic-to-linear topological transformation of polymer chains and subsequent reassembly of the linear polymers.

Taken together, C2 micelles were thus screened as an optimal formulation for subsequent in vitro controlled release applications and evaluations due to the smallest particle size with the best colloidal stability. The morphology of self-assembled micelles was observed by transmission electron microscopy (TEM) measurements. Both C2 and L2 micelles formed well-dispersed spherical nanoparticles with uniform sizes. The average diameters of C2 and L2 micelles observed by TEM are estimated to be around 50−60 and 70−80 nm, respectively (Figure S14).

Doxorubicin (DOX) was next used as a model drug to be physically loaded into the hydrophobic cores of C and L micelles via dialysis (Figure S15). DOX-loaded micelles showed particle sizes larger than those of the blank micelles owing to DOX encapsulation.[31] More importantly, DOX-loaded C2 and L2 micelles exhibited excellent salt stability, as evidenced by the almost constant particle sizes in PBS (7.4), irrespective of incubation for 24 and 48 h. The drug-loading content (DLC) and entrapment efficacy (EE) of L2@DOX and C2@DOX micelles were determined by the UV/vis spectrophotometer based on the standard DOX calibration curves to be 4.4% and 41.9%, 5.2% and 45.7%, respectively. The greater drug loading capacity of C2 micelles in comparison to that of L2 micelles is feasibly associated with the different stacking behaviors due to the topological differences. The stronger spatial resistance between the cyclic polymer chains in comparison to that of the linear ones enables the cyclic polymer chains to have stronger hydrophobic interactions with DOX for significantly improved drug loading capacity.

In vitro drug release behaviors were subsequently investigated in a physiological pH of 7.4, an intracellular acidic pH of 5.0 with/without UV irradiation (Figure S16). Incubation at pH 7.4 led to 33% and 27% DOX release in 72 h for the L2@DOX and C2@DOX micelles, respectively. The C2@DOX micelles showed a cumulative drug release lower than that of the L2@DOX micelles likely attributed to the stronger colloidal stability of C2 micelles for better drug encapsulation and slower drug diffusion. However, incubation at pH 5.0 resulted in greater cumulative drug release amounts of approximately 57% and 61% in an identical duration of 72 h for L2@DOX and C2@DOX micelles, respectively, which is attributed to the hydrophobic-to-hydrophilic changes of the PDMAEMA core for micelle destruction and promoted drug diffusion. Simultaneous exertion of an acidic pH and UV irradiation, i.e., incubation at pH 5.0 for 12 h followed by UV

https://doi.org/10.1021/acsmacrolett.3c00265
ACS Macro Lett. 2023, 12, 1025−1030

irradiation for 0.5 h promoted the cumulative drug release amount to about 78% in the same duration, suggesting apparently a faster drug release behavior for C2 micelles under acidic pH/UV light dual triggers. Most importantly, the results validate that cyclic-to-linear topological modulation is a useful strategy to promote drug release for cyclic polymer-based delivery vehicles due to the lower colloidal stability of the linear polymers. In contrast, the cumulative drug release of L2 micelles was substantially unchanged irrespective of UV irradiation, which was consistent with the above UV irradiation-independent micellar sizes.

In vitro endocytosis properties of L2@DOX and C2@DOX micelles in hepatocellular carcinoma Bel-7402 cells was visualized by fluorescence microscopy (Figure 3), and the

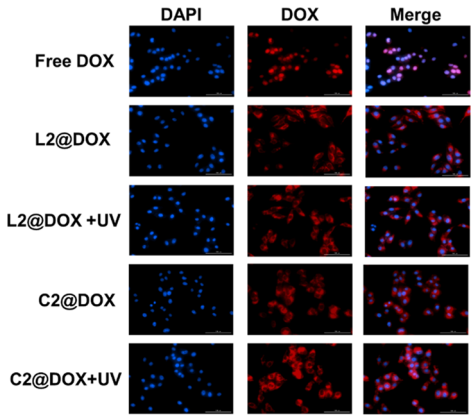

Figure 3. Fluorescence images of free DOX, micelles of L2@DOX, C2@DOX, L2@DOX + 5 min UV, and C2@DOX + 5 min uptake in Bel-7402 cells (nuclei stained blue with DAPI) for 4 h, and DOX concentration = 40 μg/mL. The scale bars represent 100 μm.

average fluorescence intensity of each group was quantified via ImageJ (Figure S17). C2@DOX and L2@DOX micelles mediated strong DOX red fluorescence close to that of free DOX in the cytoplasm after 4 h of incubation, suggesting effective intracellular DOX delivery via both micelle formulations. Significantly stronger red fluorescence was observed for the C2@DOX group than that of the L2@DOX group, suggesting probably that the cyclic copolymer-based micelles were more favorable for cellular uptake than the linear ones. Most importantly, incubation of the cells with C2@DOX and L2@DOX micelles for 2 h followed by 5 min of UV irradiation and subsequently another 2 h of incubation led to a significantly enhanced red fluorescence of DOX in the C2@DOX group, while negligible changes were observed in the L2@DOX group. The results confirm the enhanced DOX release with stronger intracellular DOX red fluorescence due to the UV irradiation-triggered cyclic-to-linear topological transformation of C2 micelles for micelle destabilization and accelerated intracellular drug release.

Finally, the in vitro cytotoxicity of various formulations was examined by [3-4,5-dimethylthiazol-2-yl]-2,5-diphenyltetrazolium bromide (MTT) cell viability assay in hepatocellular carcinoma Bel-7402 cells. The blank micelles showed a survival ratio higher than 80% even at the tested greatest polymer concentration of 2.0 mg/mL (Figure S18), demonstrating the nontoxicity of blank micelles. The almost unaltered cell viability upon UV irradiation further confirmed that the photolyzed products of blank micelles were basically nontoxic as well.

The IC_{50} values of Bel-7402 cells were determined to be 3.73, 3.94, 3.64, and 2.28 μg/mL (DOX equiv) for L2@DOX, C2@DOX, L2@DOX+UV, and C2@DOX+UV, respectively. L2@DOX micelles showed almost the same IC_{50} values with and without UV irradiation, but C2@DOX micelles with UV irradiation mediated an IC_{50} value 1.7-fold lower than that acquired without UV irradiation, strongly suggesting the significant role of topological transformation in enhancing the anticancer efficiency of cyclic polymer-based micelles (Figure S19).

In summary, we reported herein the preparation of pH/UV dual sensitive cyclic copolymers with UV-cleavable ONB ester links placed in the junction of the cyclic polymers. Interestingly, C2@DOX micelles with UV irradiation mediated a cellular uptake efficiency 1.3-fold greater as well as an IC_{50} value 1.7-fold lower than those acquired without UV irradiation, which strongly emphasizes the significant role of "cyclic-to-linear" topological transformation modulation in enhancing the anticancer efficiency of cyclic polymer-based micelles for promoted intracellular drug release. Therefore, our study highlights for the first time that topological modulation is a useful approach to promote the drug release of nanocarriers with enhanced therapeutic efficiency.

However, clinical applications of UV-responsive drug delivery systems have been greatly hampered by the inherent poor penetration ability of UV light, as well as the potential toxicity of UV irradiation to normal cells and tissues. Considering the better penetration performance of near-infrared radiation (NIR) in comparison to that of UV light, upcoming studies may include the introduction of upconverting nanoparticles to transform the UV light-sensitivity to NIR-responsiveness or synthesis of a novel NIR-responsive double-head initiator to promote practical applications of these cyclic polymer-based nanocarriers.

■ ASSOCIATED CONTENT

Supporting Information

The Supporting Information is available free of charge at https://pubs.acs.org/doi/10.1021/acsmacrolett.3c00265.

Materials and experimental details, ^{1}H NMR spectra for initiator synthesis and L polymers, ultraviolet responsive structural changes data, and in vitro cytotoxicity plots (Table S1 and Figures S1−S19) (PDF)

■ AUTHOR INFORMATION

Corresponding Authors

Cui-Yun Yu − *Hunan Province Cooperative Innovation Center for Molecular Target New Drug Study & Department of Pharmacy and Pharmacology, University of South China, Hengyang 421001, China;* orcid.org/0000-0002-2076-6228; Email: yucuiyunusc@hotmail.com

Hua Wei − *Hunan Province Cooperative Innovation Center for Molecular Target New Drug Study & Department of Pharmacy and Pharmacology, University of South China, Hengyang 421001, China*; Email: weih@usc.edu.cn

Authors

Hongbing Liu − *Hunan Province Cooperative Innovation Center for Molecular Target New Drug Study & Department*

https://doi.org/10.1021/acsmacrolett.3c00265
ACS Macro Lett. 2023, 12, 1025−1030

of Pharmacy and Pharmacology, University of South China, Hengyang 421001, China

Zheng Guo − *Hunan Province Cooperative Innovation Center for Molecular Target New Drug Study & Department of Pharmacy and Pharmacology, University of South China, Hengyang 421001, China*

Wei Ma − *Hunan Province Cooperative Innovation Center for Molecular Target New Drug Study & Department of Pharmacy and Pharmacology, University of South China, Hengyang 421001, China*

Shuang Li − *Hunan Province Cooperative Innovation Center for Molecular Target New Drug Study & Department of Pharmacy and Pharmacology, University of South China, Hengyang 421001, China*

Dun Wang − *Hunan Province Cooperative Innovation Center for Molecular Target New Drug Study & Department of Pharmacy and Pharmacology, University of South China, Hengyang 421001, China*

Zhi Zheng − *Hunan Province Cooperative Innovation Center for Molecular Target New Drug Study & Department of Pharmacy and Pharmacology, University of South China, Hengyang 421001, China*

Ying Liu − *Hunan Province Cooperative Innovation Center for Molecular Target New Drug Study & Department of Pharmacy and Pharmacology, University of South China, Hengyang 421001, China*

Complete contact information is available at: https://pubs.acs.org/10.1021/acsmacrolett.3c00265

Author Contributions

[§]H.L. and Z.G. contributed equally to this paper. CRediT: **Hongbing Liu** data curation (equal), formal analysis (equal), methodology (equal), writing-original draft (lead); **Zheng Guo** conceptualization (equal), data curation (lead), formal analysis (lead), investigation (lead), methodology (lead), software (lead), validation (lead); **Wei Ma** formal analysis (supporting), investigation (supporting), writing-original draft (supporting); **Shuang Li** data curation (supporting), formal analysis (supporting); **Dun Wang** data curation (supporting); **Zhi Zheng** data curation (supporting); **Ying Liu** data curation (supporting); **Cui-Yun Yu** funding acquisition (equal), project administration (equal), supervision (equal); **Hua Wei** conceptualization (lead), funding acquisition (lead), project administration (lead), supervision (lead), writing-original draft (lead), writing-review & editing (lead).

Notes

The authors declare no competing financial interest.

■ ACKNOWLEDGMENTS

The authors acknowledge the financial support from the Thousand Young Talent Program, the Foundation of Hunan Provincial Natural Science Foundation of China (2022JJ40381).

■ REFERENCES

(1) Morita, T.; Mukaide, S.; Chen, Z.; Higashi, K.; Imamura, H.; Moribe, K.; Sumi, T. Unveiling the Interaction Potential Surface between Drug-Entrapped Polymeric Micelles Clarifying the High Drug Nanocarrier Efficiency. *Nano Lett.* **2021**, *21*, 1303−1310.

(2) Ghezzi, M.; Pescina, S.; Padula, C.; Santi, P.; Del Favero, E.; Cantù, L.; Nicoli, S. Polymeric micelles in drug delivery: An insight of the techniques for their characterization and assessment in biorelevant conditions. *J. Controlled Release* **2021**, *332*, 312−336.

(3) Sun, X.; Wang, G.; Zhang, H.; Hu, S.; Liu, X.; Tang, J.; Shen, Y. The Blood Clearance Kinetics and Pathway of Polymeric Micelles in Cancer Drug Delivery. *ACS Nano* **2018**, *12*, 6179−6192.

(4) Rosenblum, D.; Joshi, N.; Tao, W.; Karp, J. M.; Peer, D. Progress and challenges towards targeted delivery of cancer therapeutics. *Nat. Commun.* **2018**, *9*, 1410.

(5) Kumar, P.; Kim, S.-H.; Yadav, S.; Jo, S.-H.; Yoo, S., II; Park, S.-H.; Lim, K. T. Redox-Responsive Core-Cross-Linked Micelles of Miktoarm Poly (ethylene oxide)-b-poly (furfuryl methacrylate) for Anticancer Drug Delivery. *ACS Appl. Mater. Interfaces* **2023**, *15*, 12719−12734.

(6) Silva, D.; Schirmer, L.; Pinho, T. S.; Atallah, P.; Cibrão, J. R.; Lima, R.; Afonso, J.; B-Antunes, S.; Marques, C. R.; Dourado, J.; Freudenberg, U.; Sousa, R. A.; Werner, C.; Salgado, A. J. Sustained Release of Human Adipose Tissue Stem Cell Secretome from Star-Shaped Poly (ethylene glycol) Glycosaminoglycan Hydrogels Promotes Motor Improvements after Complete Transection in Spinal Cord Injury Rat Model. *Adv. Healthcare Mater.* **2023**, *12*, 2202803.

(7) Melnyk, T.; Masiá, E.; Zagorodko, O.; Conejos-Sánchez, I.; Vicent, M. J. Rational design of poly-L-glutamic acid-palbociclib conjugates for pediatric glioma treatment. *J. Controlled Release* **2023**, *355*, 385−394.

(8) Kim, J.; Choi, S.; Baek, J.; Park, Y. I.; Kim, J. C.; Jeong, J.-E.; Jung, H.; Kwon, T.-H.; Kim, B.-S.; Lee, S.-H. Design of Topology-Controlled Polyethers toward Robust Cooperative Hydrogen Bonding. *Adv. Funct. Mater.* **2023**, 2302086.

(9) Yang, H.; Sun, L.; Chen, R.; Xiong, Z.; Yu, W.; Liu, Z.; Chen, H. Biomimetic dendritic polymeric microspheres induce enhanced T cell activation and expansion for adoptive tumor immunotherapy. *Biomaterials* **2023**, *296*, 122048.

(10) Nian, S.; Huang, B.; Freychet, G.; Zhernenkov, M.; Cai, L.-H. Unexpected Folding of Bottlebrush Polymers in Melts. *Macromolecules* **2023**, *56*, 2551−2559.

(11) Yao, H.; Li, S.-Y.; Zhang, H.; Pang, X.-Y.; Lu, J.-L.; Chen, C.; Jiang, W.; Yang, L.-P.; Wang, L.-L. Tetralactam macrocycle based indicator displacement assay for colorimetric and fluorometric dual-mode detection of urinary uric acid. *Chem. Commun.* **2023**, *59*, 5411−5414.

(12) Ma, W.; Kang, G.-Y.; Sun, L.; Meng, C.; Liu, Y.; Zheng, Z.; Jiang, M.-C.; Wang, D.; Pun, S. H.; Yu, C.-Y.; Wei, H. Multicyclic topology-enhanced anticancer drug delivery. *J. Controlled Release* **2022**, *345*, 278−291.

(13) Zhang, M.; Liu, Y.; Peng, J.; Liu, Y.; Liu, F.; Ma, W.; Ma, L.; Yu, C.-Y.; Wei, H. Facile construction of stabilized, pH-sensitive micelles based on cyclic statistical copolymers of poly (oligo (ethylene glycol) methyl ether methacrylate-st-N, N-dimethylaminoethyl methacrylate) for in vitro anticancer drug delivery. *Polym. Chem.* **2020**, *11*, 6139−6148.

(14) Haque, F. M.; Grayson, S. M. The synthesis, properties and potential applications of cyclic polymers. *Nat. Chem.* **2020**, *12*, 433−444.

(15) Yin, C.; Wang, R.; Sun, Y.; Li, S.; Zhang, X.; Gu, J.; Wu, W.; Jiang, X. The in vitro and in vivo properties of ringlike polymer brushes. *Nano Today* **2021**, *41*, 101293.

(16) Chen, C.; Singh, M. K.; Wunderlich, K.; Harvey, S.; Whitfield, C. J.; Zhou, Z.; Wagner, M.; Landfester, K.; Lieberwirth, I.; Fytas, G.; Kremer, K.; Mukherji, D.; Ng, D. Y. W.; Weil, T. Polymer cyclization for the emergence of hierarchical nanostructures. *Nat. Commun.* **2021**, *12*, 3959.

(17) Zhang, M.; Peng, X.; Ding, Y.; Ke, X.; Ren, K.; Xin, Q.; Qin, M.; Xie, J.; Li, J. A cyclic brush zwitterionic polymer based pH-responsive nanocarrier-mediated dual drug delivery system with lubrication maintenance for osteoarthritis treatment. *Materials Horizons* **2023**, *10*, 2554.

(18) Xiao, Z.; Tan, Y.; Cai, Y.; Huang, J.; Wang, X.; Li, B.; Lin, L.; Wang, Y.; Shuai, X.; Zhu, K. Nanodrug removes physical barrier to promote T-cell infiltration for enhanced cancer immunotherapy. *J. Controlled Release* **2023**, *356*, 360−372.

(19) Yan, J.; Wang, Y.; Zhang, J.; Liu, X.; Yu, L.; He, Z. Rapidly Blocking the Calcium Overload/ROS Production Feedback Loop to Alleviate Acute Kidney Injury via Microenvironment-Responsive BAPTA-AM/BAC Co-Delivery Nanosystem. *Small* **2023**, *19*, 2206936.
(20) Morgese, G.; Cavalli, E.; Rosenboom, J.-G.; Zenobi-Wong, M.; Benetti, E. M. Cyclic Polymer Grafts That Lubricate and Protect Damaged Cartilage. *Angew. Chem., Int. Ed.* **2018**, *57*, 1621−1626.
(21) Wei, H.; Wang, C. E.; Tan, N.; Boydston, A. J.; Pun, S. H. ATRP Synthesis of Sunflower Polymers Using Cyclic Multi-macroinitiators. *ACS Macro Lett.* **2015**, *4*, 938−941.
(22) Meng, C.; Cao, Y.; Sun, L.; Liu, Y.; Kang, G.; Ma, W.; Peng, J.; Deng, K.; Ma, L.; Wei, H. Synthesis of cyclic graft polymeric prodrugs with heterogeneous grafts of hydrophilic OEG and reducibly conjugated CPT for controlled release. *Biomaterials Science* **2020**, *8*, 4206−4215.
(23) Li, F.; Qin, Y.; Lee, J.; Liao, H.; Wang, N.; Davis, T. P.; Qiao, R.; Ling, D. Stimuli-responsive nano-assemblies for remotely controlled drug delivery. *J. Controlled Release* **2020**, *322*, 566−592.
(24) de Souza-Guerreiro, T. C.; Bondelli, G.; Grobas, I.; Donini, S.; Sesti, V.; Bertarelli, C.; Lanzani, G.; Asally, M.; Paternò, G. M. Membrane Targeted Azobenzene Drives Optical Modulation of Bacterial Membrane Potential. *Advanced Science* **2023**, *10*, 2205007.
(25) Abdollahi, A.; Ghasemi, B.; Nikzaban, S.; Sardari, N.; Jorjeisi, S.; Dashti, A. Dual-Color Photoluminescent Functionalized Nano-particles for Static-Dynamic Anticounterfeiting and Encryption: First Collaboration of Spiropyran and Coumarin. *ACS Appl. Mater. Interfaces* **2023**, *15*, 7466−7484.
(26) Takada, K.; Yasaki, K.; Rawat, S.; Okeyoshi, K.; Kumar, A.; Murata, H.; Kaneko, T. Photoexpansion of Biobased Polyesters: Mechanism Analysis by Time-Resolved Measurements of an Amorphous Polycinnamate Hard Film. *ACS Appl. Mater. Interfaces* **2021**, *13*, 14569−14576.
(27) Tajmoradi, Z.; Roghani-Mamaqani, H.; Salami-Kalajahi, M. Cellulose nanocrystal-grafted multi-responsive copolymers containing cleavable o-nitrobenzyl ester units for stimuli-stabilization of oil-in-water droplets. *Chemical Engineering Journal* **2021**, *417*, 128005.
(28) Kubota, H.; Ouchi, M. Rapid and Selective Photo-degradation of Polymers: Design of an Alternating Copolymer with an o-Nitrobenzyl Ether Pendant. *Angew. Chem., Int. Ed.* **2023**, *62*, e202217365.
(29) Wang, Y.; Wu, Z.; Ma, Z.; Tu, X.; Zhao, S.; Wang, B.; Ma, L.; Wei, H. Promotion of micelle stability via a cyclic hydrophilic moiety. *Polym. Chem.* **2018**, *9*, 2569−2573.
(30) Anirudhan, T. S.; Parvathy, J.; Nair, A. S. A novel composite matrix based on polymeric micelle and hydrogel as a drug carrier for the controlled release of dual drugs. *Carbohydr. Polym.* **2016**, *136*, 1118−1127.
(31) Zhuang, W.; Xu, Y.; Li, G.; Hu, J.; Ma, B.; Yu, T.; Su, X.; Wang, Y. Redox and pH Dual-Responsive Polymeric Micelles with Aggregation-Induced Emission Feature for Cellular Imaging and Chemotherapy. *ACS Appl. Mater. Interfaces* **2018**, *10*, 18489−18498.

https://doi.org/10.1021/acsmacrolett.3c00265
ACS Macro Lett. 2023, 12, 1025−1030